

Pipe corrosion and deposit study using neutron- and gamma- radiation sources

Márton Balaskó^{a,*}, Erzsébet Sváb^b, Attila Kuba^c, Zoltán Kiss^c,
Lajos Rodek^c, Antal Nagy^c

^a*KFKI Atomic Energy Research Institute, P.O. Box 49, H-1525 Budapest, Hungary*

^b*MTA SZFKI, P.O. Box 49, H-1121 Budapest, Hungary*

^c*Department of Image Processing and Computer Graphics, University of Szeged, Árpád tér 2, Szeged, H-6720, Hungary*

Available online 24 February 2005

Abstract

The problems of corrosion and deposit are crucial issues in the pipelines of the chemical, nuclear and petrochemical industries. Radiography (neutron, gamma, X-ray) has long been used as a technique for pipe inspection and corrosion monitoring. The 10 MW Budapest research reactor site is a source of various energy neutron (thermal and epithermal) and gamma radiation. The detector system was a Peltier-cooled LLL CCD camera controlled by a PC with Image ProLite software and imaging plate equipment with a BAS 2500 scanner that used AIDA software. The objects inspected were corroded tubes and various kinds of test specimens with a large wall thickness (25 mm) inside and outside steps. In the evaluation part we used tomographic algorithms. A software simulation study was made as well. Fan-beam projections were computed of the given software phantoms and a new discrete tomography method was used to reconstruct the unknown objects from these projections.

© 2005 Elsevier B.V. All rights reserved.

PACS: 81.40.Np; 81.70.Yp

Keywords: Pipeline; Neutron and gamma radiography; Software simulation; Discrete tomography

1. Introduction

The transportation of liquids and gases by pipelines is the most economical and efficient

way of delivering them where and when they are needed. Pipeline safety and reliability are of key importance for the nuclear and petrochemical industries. The condition of critical components in these industries can be monitored by the proper use of non-destructive testing methods. Preventive and corrective maintenance helps to protect the environment and the public from excessive risk of

*Corresponding author. Tel.: +36 1 392 2222;
fax: +36 1 395 9162.

E-mail address: balasko@sunserv.kfki.hu (M. Balaskó).

an industrial accident. One of the most important parameters in a pipeline to be monitored and measured is the wall thickness. Only radiographic methods may provide inspections without the costly removal of insulation material during the operation of the plant. An additional advantage is that this technique can even be applied in high-temperature environments. The principles of corrosion and wall thickness measurement/monitoring by means of tangential film-based radiography have been known for rather a long time [1,2]. Most of our experience, however, is limited to the qualitative determination of internal defects and there are no standardised and universally recognised protocols. The goal of our work is to define the optimum method and radiation source, test parameters, geometrical arrangements, and find the minimum necessary number of exposures. We would also like a more accurate interpretation and evaluation of the wall, deposit thickness and pit depth and determination of deposits in on-line piping.

A software simulation study was carried out by us to detect pipeline malformations. This study was based on a new discrete tomography (DT) method. We reconstructed the wall of the pipeline from the given projections, assuming that there was no information available about inner volumes and the pipe was surrounded by air.

2. Experimental procedure

The reactor core was the radiation source of the radiography station of the 10 MW Budapest research reactor site [3]. The neutron flux was $10^8 \text{ n cm}^{-2} \text{ s}^{-1}$ and the intensity of gamma radiation was 8.3 Gy h^{-1} . The beam of the radiography station pointed directly into the reactor core. For this reason both neutron and gamma spectra were white spectra, simultaneously containing a wide range of different energies. In addition, the nominal values of radiation intensity were not quite stable and varied, depending on the state of the reactor core. We had to repeatedly perform test exposures to obtain radiography pictures of optimal quality. Each time we had to use a 50 mm Pb filter and a reasonable exposure time, or we had

to use a 2 mm Cd filter to reduce the activation level of the object investigated during the gamma radiography (GR) work. The radiation channel contained a complex, sandwich-style collimator (diameter 25 mm) which was able to generate neutron and gamma beams simultaneously. The collimator ratio (L/D) was 190 and the diameter of the beam was 230 mm in the exposure plane. In the first case the radiography images were detected by a Photo Science Monoview type, Peltier-cooled CCD camera. A NaCs single crystal scintillation screen was used as a converter to turn gamma radiation (GR) into light flashes. A ZnS-Ag⁶Li scintillation screen was used as a converter to turn neutron radiation (NR) into flashes of light. The CCD camera data were processed by the Image ProLite software package. In the second case the radiography images were detected by BAS-SR20 × 40 imaging plates for GR exposures and were detected by BAS-ND20X40 imaging plates for NR exposures. The BAS 2500-type reader was calibrated in a separate, specially designed cabin in the reactor hall. The evaluation work was performed by an AIDA software package.

A software package was also implemented for the software simulation. It is able to generate projections and reconstruct discrete objects from the given projections as well.

3. Objects investigated

Two reference steel pipes were specially manufactured for the tests. The first one had an outer diameter of 10 in. (263 mm), 20 mm wall thickness and was 585 mm in length. The second one had an outer diameter of 13 in. (328 mm), 25 mm wall thickness and was 500 mm in length. Each reference pipe contained 7 inside and 7 outside machined steps to simulate internal and external corrosion. Each step had a length of 30 mm and the wall thickness was chosen from 6–20 mm in 2 mm steps on the 10 in. pipe. The wall thickness was chosen from 7.5–25 mm in 2.5 mm steps on a 12 in. pipe. The test blocks had inside and outside holes. The diameter of the holes was equal to the remaining wall thickness. The depths of the holes were 10, 20 and 50% of the step thickness spaced

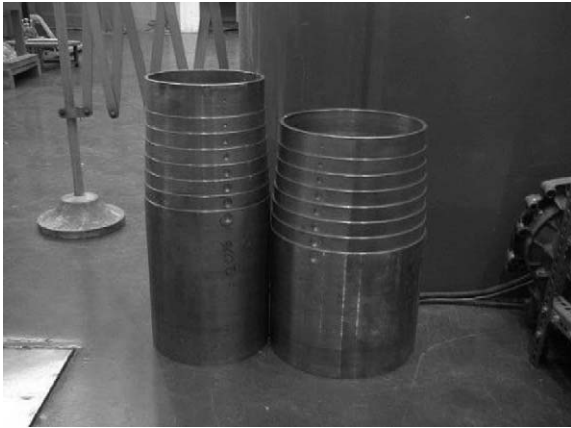


Fig. 1. Photo of the two reference blocks.

at different positions separated by 120° , and the holes had flat bottoms. Where the steps were located on the inside surface of the pipe, the material was removed by an electric spark machine to a depth of 15% of the maximum wall thickness of the pipe, which produced a flat surface. The steps covered the length of each pipe. The separation was 60° from the nearest holes. The precision was $\pm 1\%$. When the steps were located on the outside surface of the pipe, material was removed by drilling with a 20–25 mm diameter tool, parallel to the pipe's axis, to a depth of 15% of the maximum wall thickness of the pipe. A photo of the two reference pipes is shown in Fig. 1.

4. Method

In the tangential radiography technique, a view of the pipe cross-section—including a view of the pipe wall—is projected on the film, allowing direct measurements of the pipe wall thickness to be made. As is shown in Fig. 2, this may be used depending on the pipe's outside diameter (OD), source-to-film distance (SFD) and the accessibility of the area to be tested.

The equivalent exposed thickness of the pipe should be determined in advance to select the most convenient gamma-ray source. The maximum penetration depth (t_{\max}) can be determined geometrically and just depends on the OD and inside

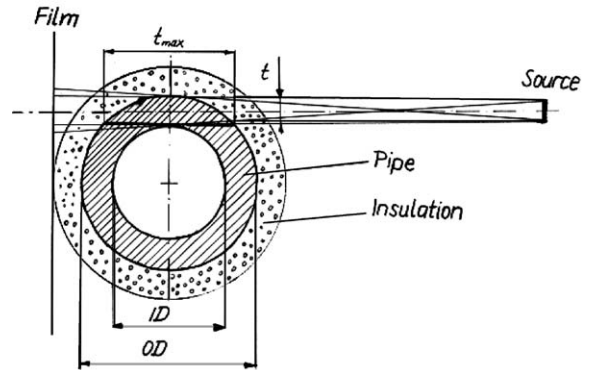


Fig. 2. Set-up for the tangential radiography tests.

diameter (ID) of the pipe. It is given by the following formula:

$$t_{\max} = \sqrt{(OD)^2 - (ID)^2}.$$

The magnification correction (MC) is

$$MC = 1 - OD/2 \text{ SFD}$$

where SFD is the focal distance.

$$MC \text{ on } 10 \text{ in. tube} = 1 - 263/2 \times 5000 = 0.9737$$

$$MC \text{ on } 12 \text{ in. tube} = 1 - 328/2 \times 5000 = 0.9672.$$

The geometrical unsharpness (U_g) is

$$U_g = F \times OD/(2\text{SFD} - OD)$$

where F is the focus size.

$$U_g \text{ on } 10 \text{ in. tube}$$

$$= 25 \times 263/2 \times 5000 - 263 = 0.68 \text{ mm}$$

$$U_g \text{ on } 12 \text{ in. tube}$$

$$= 25 \times 328/2 \times 5000 - 328 = 0.85 \text{ mm.}$$

5. Experimental tests

5.1. Experimental tests with the CCD camera

The double Peltier-cooled CCD camera was situated far from the scattered radiation source behind 100 mm Pb shielding at the radiography station. It was equipped with a remote-controlled

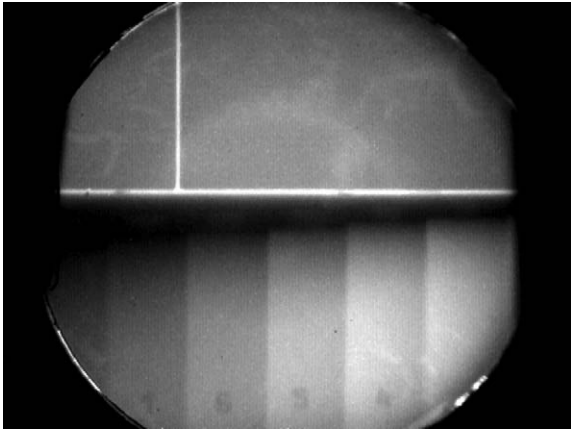


Fig. 3. Gamma radiography CCD camera image on the 10 in. tube for inside steps 7 to 1.

zoom optics system to optimise the optical parameters of the radiography pictures. The resolution of the camera was 512×512 lines and its dynamics was 10 bits. A reasonable picture was produced with a 100 video picture frame time (4 s), applying a NaCs single crystal scintillator screen like that shown in Fig. 3 on the inside steps on the 10 in. reference tube (the maximum penetration thickness was 140 mm).

5.2. Experimental work with imaging plate (IP) technique

The BAS-SR20X40 IPs were used for GR and BAS-ND20X40 type IP was employed for NR. Both IPs were applied to the same screen system as that used for the X-ray films. As regards the high-intensity gamma and neutron radiation of the beam at the radiography station, the exposure time was about 90 s using a 100 mm Pb filter on the inside steps of a 10 in. reference tube. One of these pictures is shown in Fig. 4, where the exposure time was 80 s and the size of the *.bmp type file was 15 MB. The size of the original *.img file was 40 MB and was processed by the AIDA software package.

In parallel with this, a preliminary exposure was made using a neutron beam on a BAS-ND20X40 IP. Both direct and transfer (employing an In-foil) techniques were used. The exposure time for the direct mode was 2 min and for the transfer mode

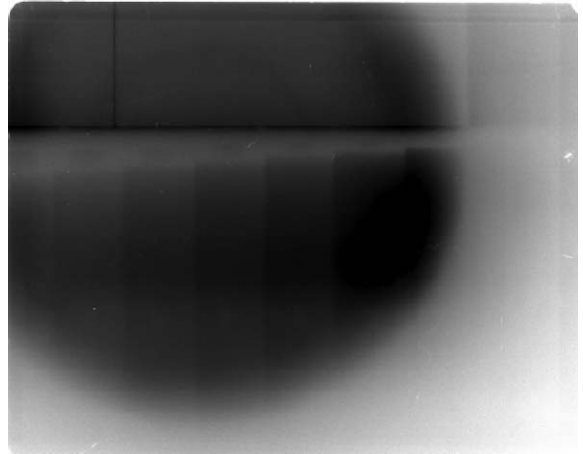


Fig. 4. Gamma radiography IP picture on the 10 in. tube for inside steps 7 to 1.

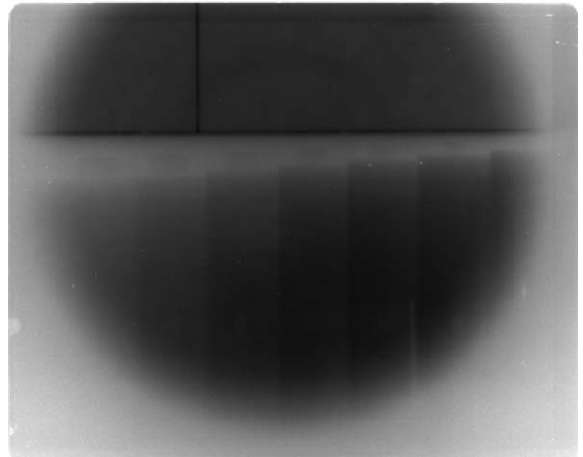


Fig. 5. A direct neutron radiography IP picture of the 10 in. tube.

was 60 + 60 min, behind a 100 mm Pb filter. Quite clearly, the quality and efficiency of the direct mode were both significantly better. Fig. 5 shows the direct NR picture of inside steps on the 10 in. reference tube.

6. Software simulation studies

Besides the method described in Section 4 and the physical experiments presented in the next

section, we decided to perform software tests using a new DT method.

First, we created geometric ring phantoms for simulating the cross-sections of the pipes with different wall thicknesses like those described in Section 3. These ring phantoms also have corresponding holes, but here they are located on the outside surface of the pipe.

Fan-beam projections of the phantoms were then computed. We supposed that the attenuation in the inner volume of the pipe was so high that the rays were totally absorbed. That is, the projections along the straight lines intersecting the inner volume are 0. In this way the rays passing through the wall of the pipe can be used for the reconstruction part. It means as well, that we have no information about the inner volume; hence we did not try to reconstruct it. What we did was reconstruct the wall of the pipe with corrosion defects. Then we could apply DT methods [4] as there were only two known materials in the object to be reconstructed: the pipe and the air. We used a DT reconstruction approach that minimized the cost function between the measured data and the projections using the general optimization strategy of simulated annealing [5].

6.1. Phantoms and projections

The thicknesses of the walls were 7, 9, 11, and 13 mm, respectively and the sizes of the holes in the wall were 7 mm × 4 mm, 9 mm × 5 mm, 11 mm × 6 mm, and 13 mm × 7 mm, respectively.

120 projections of the software phantoms were uniformly taken around the whole circle. The projections were calculated using strip integrals. The angle between the projections was 6°, and the distance of detector from the origin was 303 mm. In order to simulate similar ray paths like those in the physical experiments, the source was placed 1000 m far away from the origin. The detector size was 400 mm and 401 samples were taken for each projection.

In the reconstruction algorithm we used only those rays that did not intersect the inner part of the ring (see Fig. 6).

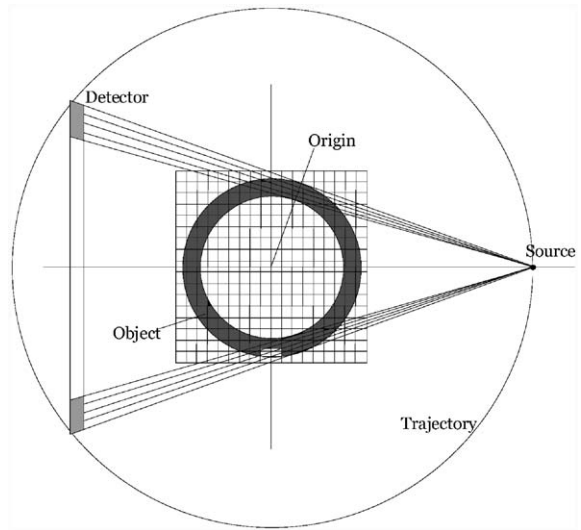


Fig. 6. Simulation of the fan-beam projections in the simulation studies. Only the grey detector positions were used for the reconstruction.

6.2. Simulation results

During this simulation we studied the following cases:

- How the reconstruction algorithm behaved if Gaussian noise was added.
- Whether we could get better result if the initial image was a perfect ring. We called this case a reconstruction using an initial prototype image. (Otherwise, the initial image was a blank image full of 0's.)

Hence the simulation was divided into two main parts: the results with and without the prototype image. We also investigated what happened if there was no noise or if there was a 5% or 10% Gaussian noise component in the projections.

The inner parts of the rings were not reconstructed as they randomly contained binary values (see Fig. 7). (As we mentioned earlier, the area and projections of the inner circle were not included in the calculation of the cost function.)

It is obvious that if the depth of the ring and size of the holes are larger, then the holes can be seen more distinctly.

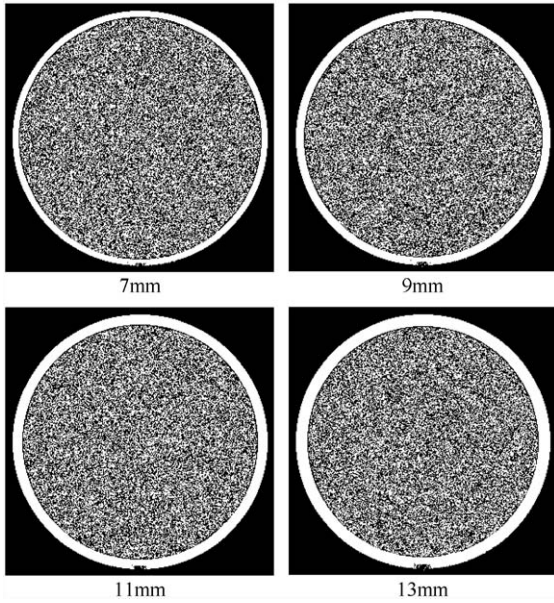


Fig. 7. Reconstruction results using prototype rings without noise.

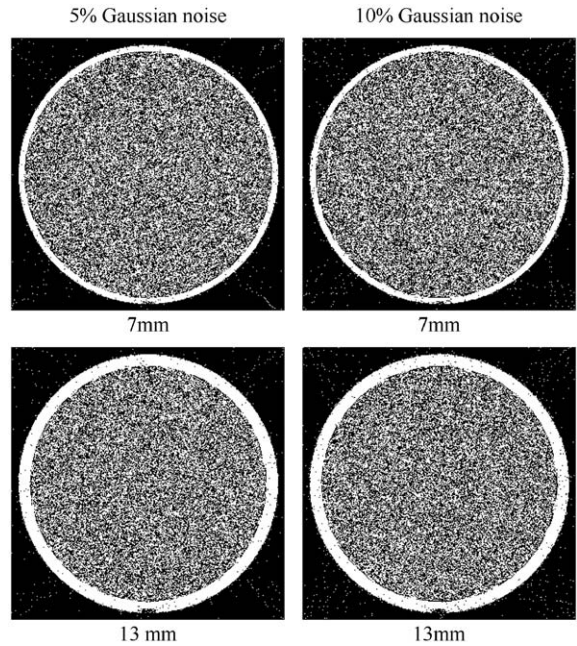


Fig. 8. Noise effects on different depth of rings. A ring prototype was used during the reconstruction.

When Gaussian noise was added, the smaller holes were detectable, but they were not as clean as in the noiseless case (see Fig. 8, first row). We obtained better results when the depth of the software phantom was larger (see Fig. 8, second row).

The results obtained were almost the same as those obtained when we did not use prototype rings during the reconstruction method.

7. Summary

We successfully manufactured two large diameter tubes, as specified by the project. The environment for performing three types of radiography experiments using the Imaging Plate technique and CCD camera—were developed at the Budapest research reactor site using both gamma- and neutron-radiation sources. The main characteristics of these techniques are summarised in Table 1.

The software simulation also yielded several interesting results. The software phantoms were reconstructed from a limited amount of available information using our new DT method. We also

Table 1
Summary of the main parameters of the imaging techniques applied

Technique	Imaging Plate	CCD camera
Exposure time	1–2 min	4–5 s
Resolution	~0.05 mm	~0.3 mm
Extra service	None	None
Evaluation	PC contributed	PC contributed
Archivation	Digitalised	Digitalised
Price	Very expensive	Expensive

carried out experiments using noiseless and noisy projections. Further investigations are necessary on the reconstruction procedure used to get better results in the future.

Acknowledgments

This work was funded by IAEA Research Contract no. HUN-12109. It was also supported by the NSF grant DMS 0306215 (Aspects of Discrete Tomography).

References

- [1] U. Zscherpel, C. Belln, Wall thickness estimation from digitized radiographs, in: B. Larsen (Ed.), Proceedings of the 7th European Conference on Non Destructive Testing (ECNDT'98), Copenhagen, 1998, pp. 2819–2825.
- [2] U. Zscherpel, Y. Onel, U. Evert, New concepts for corrosion inspection of pipelines by digital industrial radiology, in: G. Nardoni (Ed.), Proceedings of the 15th World Conference on Non Destructive Testing (WCNDT'2000), Rome, 2000 idn.325. htm, 8p.
- [3] M. Balasko, E. Svab, Nucl. Instr. and Meth. A 377 (1996) 140.
- [4] G.T. Herman, A. Kuba (Eds.), Discrete Tomography, Foundations, Algorithms, and Applications, Birkhäuser, Boston, 1999.
- [5] N. Robert, F. Peyrin, M.J. Yaffe, Med. Phys. 21 (1994) 1839.